

Unusual Photophysics of a Rhenium(I) Dipyridophenazine Complex in Homogenous Solution and Bound to DNA

Heather D. Stoeffler, Nancy B. Thornton, Stacy L. Temkin, and Kirk S. Schanze*

Contribution from the Department of Chemistry, University of Florida, P.O. Box 117200, Gainesville, Florida 32611-7200

Received November 14, 1994[⊗]

Abstract: The photophysics of [*fac*-(dppz)Re^I(CO)₃(4-MePy)][Cl] (**1**, where dppz = dipyrido[3,2-*a*:2',3'-*c*]phenazine and 4-MePy = 4-methylpyridine) have been examined in organic solvents and in aqueous solution with and without calf thymus DNA. Emission and nanosecond to microsecond transient absorption studies of **1** in organic solvents such as MeOH, MeCN, and CH₂Cl₂ indicate that the lowest excited state of the complex is a dppz-based intraligand triplet state (³IL_{dppz}). The ³IL_{dppz} state is characterized by weak room temperature phosphorescence and a strong T₀ → T_n absorption band with λ_{max} = 470 nm. Absorption and emission studies of **1** in aqueous solution with added DNA indicate that the complex binds to the biopolymer, presumably by intercalation of the dppz ligand. Complex **1** is non-luminescent in aqueous solution; however, ³IL_{dppz} phosphorescence is observed from the DNA-bound form of the complex in aqueous solution. The ³IL_{dppz} assignment for the emission from the DNA-bound complex is supported by the observation of the characteristic T₀ → T_n transient absorption feature at 470 nm in the absorption-difference spectrum of the DNA-bound complex.

Introduction

The unique physicochemical properties of transition metal complexes have provided an avenue for the development of a remarkably diverse new class of molecular probes for exploring and/or modifying the structure of DNA.^{1,2} Much of the work in this area stemmed from the early studies of Pt(II) complexes that were motivated, in part, by a desire to understand the mechanism of action of *cis*-platin and related chemotherapeutic agents.^{3–7} However, the recent explosive growth of this area has been driven largely by the recognition that a wide array of transition metal complexes of Ru(II), Rh(III), and Cu(I) with polynuclear aromatic chelate ligands such as 1,10-phenanthroline interact strongly with DNA and provide a diverse set of physical and chemical tools for probing and modifying the structure of nucleic acids.^{2,8–16}

A particular area that has received considerable recent attention concerns the exploration of the interaction between

double-stranded DNA and transition metal complexes that feature the ligand dipyrido[3,2-*a*:2',3'-*c*]phenazine (dppz).^{16–23} These systems are of interest because dppz complexes bind strongly to DNA, presumably via intercalation of the dppz ligand. Furthermore, in many cases intercalative binding to DNA leads to a profound change in the photophysical properties of transition metal dppz complexes.¹⁹ Initial studies which examined the interaction of (bpy)₂Ru^{II}(dppz)²⁺ (bpy = 2,2'-bipyridine) and related complexes with various forms of DNA led to several important conclusions.^{19–21} First, in (bpy)₂Ru^{II}(dppz)²⁺, the lowest excited state apparently arises from a metal-to-ligand charge transfer (MLCT) transition in which the ligand-based orbital that is involved is localized on dppz (e.g., the transition is dominated by the configuration dτ_{Ru}⁵π*_{dppz}¹). Second, this luminescent ³MLCT excited state, ³(bpy)₂Ru^{III}(dppz^{•-})^{2+*}, is strongly quenched in aqueous solution, presumably by proton transfer (or H-bond formation) from H₂O to one of the phenazine nitrogens in the dppz ligand.^{19,20} Third, the aqueous solvent-induced quenching of the luminescent ³MLCT state is strongly suppressed when the complex binds to DNA, leading to the property that the complex is luminescent only when bound to DNA.^{19,20} This unique property provides the basis for a series of transition metal complexes that can be used as luminescent reporters for binding to double-stranded DNA.^{19,20}

[⊗] Abstract published in *Advance ACS Abstracts*, June 15, 1995.

- (1) Tullius, T. D. Ed. *Metal-DNA Chemistry*; American Chemical Society: Washington, DC, 1989.
- (2) Pyle, A. M.; Barton, J. K. *Prog. Inorg. Chem.* **1990**, *38*, 412.
- (3) Lippard, S. J. *Acc. Chem. Res.* **1978**, *11*, 211.
- (4) Lippard, S. J., Ed. *Platinum, Gold, and Other Metal Chemotherapeutic Agents*; American Chemical Society: Washington, DC, 1983.
- (5) Barton, J. K.; Lippard, S. J. *Met. Ions Biol.* **1980**, *1*, 31.
- (6) Sherman, S. E.; Lippard, S. J. *Chem. Rev.* **1987**, *87*, 1153.
- (7) Kopf-Maier, P.; Kopf, H. *Chem. Rev.* **1987**, *87*, 1137.
- (8) Barton, J. K.; Dannenberg, J. J.; Raphael, A. L. *J. Am. Chem. Soc.* **1982**, *104*, 4967.
- (9) Barton, J. K.; Danishefsky, A. T.; Goldberg, J. M. *J. Am. Chem. Soc.* **1984**, *106*, 2172.
- (10) Barton, J. K.; Goldberg, J. M.; Kumar, C. V.; Turro, N. J. *J. Am. Chem. Soc.* **1986**, *108*, 2081.
- (11) Pyle, A. A.; Long, E. C.; Barton, J. K. *J. Am. Chem. Soc.* **1989**, *111*, 4520.
- (12) Tamilarasan, R.; McMillin, D. R. *Inorg. Chem.* **1990**, *29*, 2798.
- (13) Mahnken, R. E.; Billadeau, M. A.; Nikonowicz, E. P.; Morrison, H. *J. Am. Chem. Soc.* **1992**, *114*, 9253.
- (14) Grover, N.; Gupta, N.; Thorp, H. H. *J. Am. Chem. Soc.* **1992**, *114*, 3390.
- (15) (a) Grover, N.; Thorp, H. H. *J. Am. Chem. Soc.* **1991**, *113*, 7030. (b) Gupta, N.; Grover, N.; Neyhart, G. A.; Singh, P.; Thorp, H. *Inorg. Chem.* **1993**, *32*, 310. (c) Kalsbeck, W. A.; Thorp, H. H. *J. Am. Chem. Soc.* **1993**, *115*, 7146.

(16) Carlson, D. L.; Huchital, D. H.; Mantilla, E. J.; Sheardy, R. D.; Murphy, W. R., Jr. *J. Am. Chem. Soc.* **1993**, *115*, 6424.

(17) Chambron, J.-C.; Sauvage, J.-P.; Amouyal, E.; Koffi, P. *New J. Chem.* **1985**, *9*, 527.

(18) Amouyal, E.; Homs, A.; Chambron, J.-C.; Sauvage, J.-P. *J. Chem. Soc., Dalton Trans.* **1990**, 1841.

(19) Friedman, A. E.; Chambron, J.-C.; Sauvage, J.-P.; Turro, N. J.; Barton, J. K. *J. Am. Chem. Soc.* **1990**, *112*, 4960.

(20) (a) Hartshorn, R. M.; Barton, J. K. *J. Am. Chem. Soc.* **1992**, *114*, 5919. (b) Jenkins, Y.; Friedman, A. E.; Turro, N. J.; Barton, J. K. *Biochemistry* **1992**, *31*, 10809. (c) Holmlin, R. E.; Barton, J. K. *Inorg. Chem.* **1995**, *34*, 7.

(21) Fees, J.; Kaim, W.; Moscherosch, M.; Matheis, W.; Klima, J.; Krejcik, M.; Zalis, S. *Inorg. Chem.* **1993**, *32*, 166.

(22) Gupta, N.; Grover, N.; Neyhart, G. A.; Liang, W.; Singh, P.; Thorp, H. H. *Angew. Chem., Int. Ed. Engl.* **1992**, *31*, 1048.

(23) Hiort, C.; Lincoln, P.; Norden, B. *J. Am. Chem. Soc.* **1993**, *115*, 3448.

We have been actively involved in examining the photo-physical and photochemical properties of a wide range of d⁶ transition metal complexes of the type *fac*-(diimine)Re^I(CO)₃-(L)⁺ (where diimine refers to a bidentate diimine ligand such as 2,2'-bipyridine and L is a monodentate ligand such as pyridine).²⁴⁻²⁸ This family of complexes typically features a moderately long-lived and strongly luminescent lowest lying excited state which is based on dπ(Re) → π* (diimine) MLCT.²⁹⁻³¹ Indeed, with respect to excited state properties this family of Re(I) complexes bears a close similarity to the prototype for MLCT excited states, (bpy)₃Ru(II), with the exception of subtle differences in excited state energy and non-radiative decay rates.³¹ Despite the strong similarities in these systems, an important distinction for the Re(I) complexes is that owing to the presence of only a single "chromophoric" diimine ligand, there is no ambiguity with respect to the acceptor ligand that is involved in the MLCT transition.³¹

In the study that is the focus of this report we have examined the photophysical properties of the complex *fac*-(dppz)Re^I(CO)₃-(4-methylpyridine)¹⁺ (**1**) in protic and aprotic organic solvents and in aqueous solution in the presence of calf thymus DNA. The motivation behind this effort was several-fold. First, because there is only one chromophoric ligand in **1**, there is no ambiguity concerning the involvement of other energetically close-lying MLCT excited states (based on other π-acceptor ligands) in the photophysics of the complex. This feature provides a unique opportunity to provide information on the basis for the unusual, and sometimes unpredictable, properties of the mixed ligand Ru(II)-dppz analogs.^{20a} Second, due to the presence of the dppz ligand and the cationic charge of the complex, it was anticipated that **1** would bind to DNA by intercalation, in direct analogy with the Ru(II)-dppz analogs. This would afford the possibility for examining the effect that intercalation with DNA would have on the photophysics of the complex.

The results of this study demonstrate that complex **1** displays remarkable photophysical properties. Unequivocal evidence is presented which indicates that the lowest excited state of **1** is a dppz-based intraligand triplet state. The dppz-based triplet state is non-luminescent in degassed aqueous solution; however, the phosphorescence yield increases dramatically when **1** binds to DNA. The basis for the unusual photophysical behavior of this complex in organic solvents as well as in the presence of DNA is discussed in detail in the succeeding sections of this report.

Experimental Section

Materials and Apparatus. Reagent grade solvents and chemicals were used without purification unless otherwise noted. Silica gel (Merck, 230-400 mesh) and neutral alumina (Fisher, Brockman grade III) were used for chromatography. NMR spectra were obtained on a General Electric QE-300 MHz spectrophotometer.

***fac*-(1,10-phenanthroline-5,6-dione)Re^I(CO)₃Cl (**4**).** A suspension of Re(CO)₅Cl³² (240 mg, 0.66 mmol) and 1,10-phenanthroline-5,6-dione²³ in toluene (7 mL) was stirred and refluxed under N₂ for 4 h.

(24) Schanze, K. S.; Cabana, L. A. *J. Phys. Chem.* **1990**, *94*, 2740.

(25) Perkins, T. A.; Humer, W.; Netzel, T. L.; Schanze, K. S. *J. Phys. Chem.* **1990**, *94*, 2229.

(26) MacQueen, D. B.; Schanze, K. S. *J. Am. Chem. Soc.* **1991**, *113*, 7470.

(27) MacQueen, D. B.; Eyster, J. R.; Schanze, K. S. *J. Am. Chem. Soc.* **1992**, *114*, 1897.

(28) Schanze, K. S.; MacQueen, D. B.; Perkins, T. A.; Cabana, L. A. *Coord. Chem. Rev.* **1993**, *122*, 63.

(29) (a) Wrighton, M.; Morse, D. L. *J. Am. Chem. Soc.* **1974**, *96*, 998.

(b) Giordano, P. J.; Wrighton, M. S. *J. Am. Chem. Soc.* **1979**, *101*, 2888.

(30) Worl, L. A.; Duesing, R.; Chen, P.; Della Ciana, L.; Meyer, T. J. *J. Chem. Soc., Dalton Trans.* **1991**, 849.

(31) Striplin, D. R.; Crosby, G. A. *Chem. Phys. Lett.* **1994**, *221*, 426.

(32) *Inorg. Synth.* **1985**, *23*, 42.

After this time the solution was cooled to 25 °C and an orange-brown solid was collected by suction filtration. The crude product was purified by chromatography on silica gel using THF as an eluant. The final product was obtained as an orange-brown microcrystalline solid, yield 230 mg (69%). ¹H NMR (300 MHz, CD₃CN) δ 7.85 (t, 2H), 8.80 (d, 2H), 9.22 (d, 2H).

***fac*-(dppz)Re^I(CO)₃Cl (**5**).** A solution of **4** (310 mg, 0.6 mmol) in absolute ethanol (15 mL) was purged with N₂. This solution was then heated with stirring to reflux, whereupon *o*-phenylenediamine (80 mg, 0.72 mmol) was added. The resulting solution was refluxed for an additional 1-h period and then cooled, whereupon **5** precipitated from the solution as a red-brown microcrystalline solid. The product was collected by suction filtration and dried in vacuum, yield 285 mg (81%). ¹H NMR (300 MHz, CD₃CN) δ 8.04 (m, 2H), 8.09 (m, 2H), 8.48 (m, 2H), 9.48 (d, 2H), 9.89 (d, 2H).

[*fac*-(dppz)Re^I(CO)₃(4-methylpyridine)][Cl] (1**).** Complex **5** (160 mg, 0.27 mmol) was added to 23 mL of dry DMF and the resulting suspension was purged with N₂ and then heated to 50 °C with stirring. At this time AgPF₆ (280 mg, 1.1 mmol) was added. Five minutes after addition of AgPF₆ a solution of 4-methylpyridine (290 μL, 3.0 mmol) in 3 mL of dry DMF was added and the resulting reaction mixture was heated to 70 °C and stirred under N₂ for 6 h. After this period the solution was filtered through a fritted glass disk with the aid of a vacuum to remove the AgCl precipitate. The DMF solvent was removed under vacuum and the resulting yellow-brown solid was purified by chromatography on silica gel eluting with MeCN/CHCl₃ (1:9 v/v). After chromatography the product was recrystallized from Et₂O/MeCN. The product of the synthesis and chromatographic purification was obtained as a yellow microcrystalline PF₆⁻ salt, yield 150 mg (69%). The PF₆⁻ salt was metathesized to the Cl⁻ form using the following procedure. A 5.0-g sample of Dowex 1X2-100 anion exchange resin was soaked in 50 mL of MeOH overnight and then loaded into a 1 cm diameter chromatography column. The Dowex column was flushed with 50 mL of 0.1 M tetramethylammonium chloride in MeOH and subsequently with 100 mL of MeOH. Then a solution of 20 mg of [(dppz)Re^I(CO)₃-(4-methylpyridine)][PF₆] in 5 mL of MeOH was added to the column and eluted using MeOH. The solution containing the product was collected and the MeOH was removed under vacuum to yield **1** as an amorphous yellow solid, yield ca. 20 mg. (The following spectroscopic data were obtained by using the PF₆⁻ salt of the complex.) ¹H NMR (300 MHz, CD₃CN) δ 2.16 (s, 3H), 7.06 (d, 2H), 8.08 (m, 2H), 8.17 (d, 2H), 8.24 (m, 2H), 8.35 (m, 2H), 9.65 (d, 2H), 9.76 (d, 2H). ¹³C NMR (75 MHz, CD₃CN) δ 19.6, 127.0, 128.2, 129.2, 130.5, 132.4, 136.4, 138.9, 142.3, 148.4, 151.0, 152.4, 155.3. HRMS (POS-FAB) calcd for C₂₇H₁₇N₅O₃Re (M⁺) 646.089, found 646.083; calcd for C₂₁H₁₀N₄O₃Re (M⁺ - pyridine) 553.031, found 553.028.

[*fac*-(phen)Re^I(CO)₃-(4-(benzoylamino)methyl)pyridine)][Cl] (2**).** This complex was prepared following an established literature procedure.²⁶ The PF₆⁻ salt was metathesized to the Cl⁻ form as described above for complex **1**. (The following spectroscopic data were obtained by using the PF₆⁻ salt of the complex.) ¹H NMR (300 MHz, CD₃CN) δ 4.39 (d, 2H), 7.13 (d, 2H), 7.48 (m, 4H), 7.72 (d, 2H), 8.10 (q, 2H), 8.19 (m, 4H), 8.83 (d, 2H), 9.60 (d, 2H).

Dipyrido[3,2-*a*:2',3'-*c*]phenazine (3**).** This compound was prepared according to a literature procedure and purified by repeated recrystallization from ethanol.³³

Preparation of Solutions Used in Spectroscopic Experiments. Organic solvents were of spectroscopic grade and were used without purification unless otherwise noted. Water was triply distilled in a glass apparatus. Buffer solutions were prepared by dissolving 3.02 g (25 mmol) of tris(hydroxymethyl)aminomethane hydrochloride (Tris) in 1 L of H₂O. The pH of the solution was then adjusted to 7.0 by dropwise addition of 20% aqueous NaOH.

Calf thymus DNA (Type I, Sigma Chemical Co.) stock solutions were prepared by dissolving approximately 50 mg of DNA in 1.5 mL of aqueous buffer solution. After mixing, the DNA solution was allowed to stand overnight at 4 °C. On the following day the solution was agitated by repeated passage through a 22 gauge syringe needle. The concentration of the stock solution was determined by diluting several aliquots to 10 mL total volume and checking the absorption at

(33) Dickeson, J. E.; Summers, L. A. *Aust. J. Chem.* **1970**, *23*, 1023.

260 nm. The concentration was evaluated by assuming the molar absorptivity per nucleotide base is $6.6 \text{ mM}^{-1} \text{ cm}^{-1}$ at 260 nm.³⁴

Titration experiments were performed by placing a 3-mL aliquot of an aqueous buffer solution containing **1** into a fluorescence cuvette which was then sealed with a septum cap. The cuvette was degassed by purging with a slow stream of argon for 30 min via a needle inserted through the septum. Absorption and/or emission spectra as a function of [DNA] were obtained by addition of μL aliquots of the DNA stock solution to the cuvette with the aid of a syringe. The solution was degassed again subsequent to the addition of each aliquot of DNA by gently bubbling for 5 min.

Solutions for transient absorption experiments were contained in a 100 mL recirculating flow cell. The concentration of each sample was adjusted such that the absorption at the laser excitation wavelength (355 nm) was 0.5 for a 1 cm path length cell and each solution was degassed while recirculating for 45 min by bubbling with argon.

Equipment and Techniques Used for Spectroscopic Experiments. UV-visible spectra were obtained using an HP-8452A diode array spectrophotometer. Corrected steady-state emission spectra were recorded on a SPEX F-112 fluorimeter. Samples were contained in degassable 1 cm \times 1 cm quartz cuvettes and the optical density was adjusted to approximately 0.1 at the excitation wavelength. Emission quantum yields are reported relative to $[\text{Ru}(\text{bpy})_3][\text{Cl}]_2$ in degassed aqueous solution ($\Phi_{\text{em}} = 0.055$)³⁵ and appropriate correction was applied for the difference in refractive indices of the sample and the actinometer solvents. Emission lifetimes were determined by time-correlated single-photon counting (FLI, Photochemical Research Associates). The excitation and emission wavelengths were selected by band-pass filters (excitation, Schott UG-11; emission, 550 nm interference filter). Lifetimes were calculated by using the DECAN deconvolution software on an 80286 microcomputer.³⁶

Transient absorption experiments were carried out using an instrument that has been described in a previous publication.³⁷ Samples were excited with the third harmonic output of a Q-switched Nd:YAG laser (355 nm, 10 ns fwhm) with a dose of 10 mJ/pulse.

Multiwavelength transient absorption data were subjected to global analysis by using the program SPECFIT.^{38,39} This software allows the application of singular value decomposition (factor analysis) to extract the spectral eigenvectors and the (temporal) evolutionary eigenvectors from multiwavelength transient absorption kinetic data. The results of the singular value decomposition are combined with kinetic model functions (e.g., $\text{A} \rightarrow \text{B} \rightarrow \text{C}$, etc.) that describe the concentration profiles of the absorbing species to obtain globally optimized rate constants and the absorption-difference spectra of the principal kinetic components.³⁹

Results

Synthesis of 1. Complex **1** was prepared by variation of the general procedure used for synthesis of complexes of the type *fac*-(diimine) $\text{Re}^{\text{I}}(\text{CO})_3(\text{L})^+$.^{28,29} Thus, reaction of 1 equiv of 1,10-phenanthroline-5,6-dione with $\text{Re}(\text{CO})_5\text{Cl}$ for 1 h in refluxing toluene leads to production of *fac*-(1,10-phenanthroline-5,6-dione) $\text{Re}(\text{CO})_3\text{Cl}$ (**4**). The facial diastereomer of **4** is formed exclusively by this reaction and therefore no special separation techniques are required to afford the pure stereoisomer.²⁹ This point is significant because prior studies indicate that metal complex-DNA interactions can be strongly dependent upon the stereochemistry of the metal complex.^{2,8-10,23} Complex **4** is then reacted with 1 equiv of *o*-phenylenediamine in refluxing ethanol for 1 h to produce *fac*-(dppz) $\text{Re}(\text{CO})_3\text{Cl}$

(34) Cantor, C. R.; Schimmel, P. R. *Biophysical Chemistry. Part II. Techniques for the Study of Biological Structure and Function*; Freeman: New York, 1980; p 402.

(35) Harriman, A. *J. Chem. Soc., Chem. Commun.* **1977**, 777.

(36) Boens, N.; DeRoeck, T.; Dockx, J.; DeSchryver, F. C. *DECAN* (v 1.0), 1991.

(37) Wang, Y.; Schanze, K. S. *Chem. Phys.* **1993**, 176, 305.

(38) *SPECFIT* (v 1.17), Spectrum Software Associates, Chapel Hill, NC, 1994.

(39) Stultz, L. K.; Binstead, R. A.; Reynolds, M. S.; Meyer, T. J. *J. Am. Chem. Soc.* **1995**, 117, 2520.

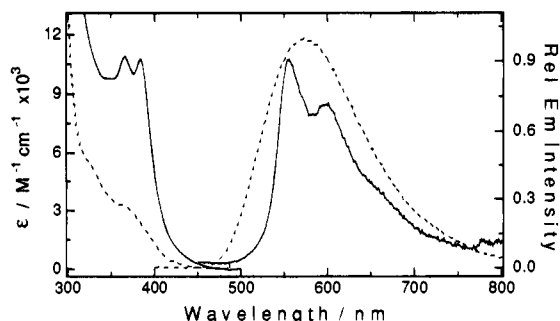
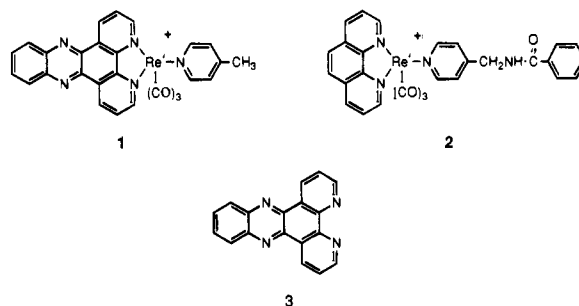


Figure 1. UV-visible absorption spectra (at left, left axis) and emission spectra (at right, right axis) of **1** and **2**. Solid line: absorption of **1** in aqueous Tris buffer and emission of **1** in degassed MeOH solution. Dashed line: absorption and emission of **2** in 30% MeOH/aqueous Tris buffer. Emission spectra of both **1** and **2** recorded with $\lambda_{\text{ex}} = 350 \text{ nm}$. Note that the y-scale for the emission spectra is arbitrary: the quantum yield for emission from **1** is ca. 100-fold lower compared to **2** (see Table 1).

(**5**) in high yield. Finally, complex **1** was prepared by treatment of **5** with AgPF_6 in warm DMF solution in the presence of a 10-fold excess of 4-picoline. This reaction occurs exclusively with retention of stereochemistry at the metal center, thereby affording the facial diastereomer of **1**. The PF_6^- salt of **1** was isolated by silica gel chromatography, characterized, and then metathesized to the Cl^- form by ion-exchange chromatography prior to the photophysical studies.

Photophysics in Homogenous Solutions. UV-visible absorption spectra of **1** and the structurally related phenanthroline complex *fac*-(phen) $\text{Re}^{\text{I}}(\text{CO})_3[4-((\text{benzoylamino})\text{methyl})\text{pyridine}]^+$ (**2**, where phen = 1,10-phenanthroline) in aqueous Tris buffer solution are compared in Figure 1. Phenanthroline complex **2** displays a broad, featureless absorption band with



$\lambda_{\text{max}} = 364 \text{ nm}$ ($\epsilon \approx 3500 \text{ M}^{-1} \text{ cm}^{-1}$) that tails weakly to 425 nm in the visible. This transition is characteristic of (diimine)- $\text{Re}^{\text{I}}(\text{CO})_3(\text{L})^+$ complexes and is assigned to the $d\pi(\text{Re}) \rightarrow \pi^*(\text{phen})$ MLCT absorption.²⁸⁻³¹ By contrast, the absorption of dppz complex **1** in the near-UV appears as a moderately intense band with two maxima at 366 and 384 nm ($\epsilon \approx 11\,000 \text{ M}^{-1} \text{ cm}^{-1}$). The absorption of the free dppz ligand (compound **3**, spectrum not shown) also appears as a band in the near-UV with two maxima at $\lambda = 358$ and 376 nm. Based on these facts, the near-UV absorption of dppz complex **1** is attributed to a superposition of the $d\pi(\text{Re}) \rightarrow \pi^*(\text{dppz})$ MLCT and the $\pi \rightarrow \pi^*(\text{dppz})$ IL transitions. This assignment implies that near-UV excitation of **1** directly populates both MLCT and π, π^* or n, π^* dppz-intraligand (IL_{dppz}) excited states.

The emission spectra of **1** in MeOH and **2** in aqueous Tris buffer are also compared in Figure 1. The emission of the phen complex appears as a broad, structureless band with $\lambda_{\text{max}} = 574 \text{ nm}$. This emission is similar to that observed from other (diimine) $\text{Re}^{\text{I}}(\text{CO})_3(\text{L})^+$ complexes and is assigned to the $d\pi(\text{Re}) \rightarrow \pi^*(\text{phen})$ ³MLCT state.²⁸⁻³¹ By contrast, emission from

Table 1. Emission Parameters for Complexes **1** and **2**^a

complex	solvent	λ/nm	$\tau_{\text{em}}/\mu\text{s}$	Φ_{em}	k_f/s^{-1}	$k_{\text{nr}}/\text{s}^{-1}$
1	CH ₂ Cl ₂	559	2.8	0.0004	1.4×10^2	3.6×10^5
	CH ₃ CN	557	18.5	0.0002	1.1×10^1	5.4×10^4
	EtOH	557	1.5	0.0005	3.3×10^2	6.7×10^5
	MeOH	556	4.3	0.003	7.0×10^2	2.3×10^5
	H ₂ O/Tris ^b	<i>c</i>	<i>c</i>	<0.00005	<i>c</i>	<i>c</i>
	H ₂ O/Tris/DNA ^d	569	0.17 (0.80) ^e	0.0006	<i>f</i>	<i>f</i>
2	CH ₃ CN	573	1.6	0.23	1.4×10^5	4.8×10^5
	EtOH	568	1.2	0.24	2.0×10^5	6.3×10^5
	MeOH	575	1.2	0.19	1.6×10^5	6.7×10^5
	H ₂ O/Tris ^b	575	1.0	0.059	5.9×10^4	9.4×10^5
	H ₂ O/Tris/DNA ^d	575	0.97	0.060	6.2×10^4	9.7×10^5

^a All experiments in argon degassed solvents at 298 K. ^b Aqueous solution of tris(hydroxymethyl)aminomethane ($c = 25$ mM), pH = 7.0. ^c Emission too weak for accurate determination. ^d Aqueous solution of tris(hydroxymethyl)aminomethane ($c = 25$ mM), pH = 7.0, with [DNA]/[1] = 15. ^e Two lifetime components from biphasic emission decay. Numbers in parentheses indicate relative amplitude of decay component. ^f Not meaningful due to biphasic emission decay.

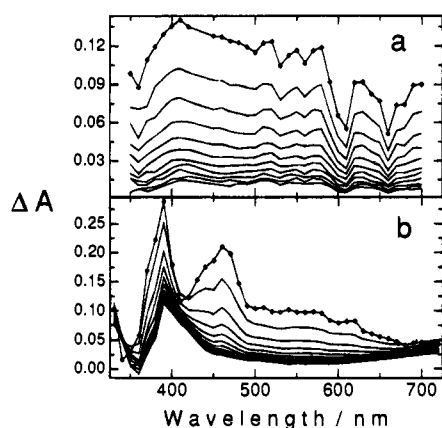


Figure 2. Transient absorption-difference spectra taken at various delay times following 355-nm laser excitation. In every set of spectra, the spectrum that is identified with point markers corresponds to 0 delay following the laser pulse. (a) Complex **2** in MeCN solution, $c = 140$ μM . Delay times range from 0 to 3.2 μs . (b) Dppz ligand **3** in MeOH solution, $c = 50$ μM . Delay times range from 0 to 16 μs .

the dppz complex in MeOH appears as a structured band with two vibronic components at $\lambda_{\text{max}} = 556$ and 598 nm. The difference in the emission spectra of **1** and **2** implies that emission from **1** may not arise from a ³MLCT state.

Emission maxima (λ_{max}), quantum yields (Φ_{em}), lifetimes (τ_{em}), and calculated radiative and non-radiative decay rates (k_f and k_{nr} , respectively) for complexes **1** and **2** were determined in several argon degassed solvents and the results are listed in Table 1. The emission parameters that are observed for phen complex **2** are very similar to those observed for a wide variety of (diimine)Re^I(CO)₃L⁺ complexes and support the assignment of the emission from this complex to the $d\pi(\text{Re}) \rightarrow \pi^*(\text{phen})$ ³MLCT excited state.^{28,30,31} By contrast, the emission parameters for dppz complex **1** are strikingly different than those of phen complex **2**. First, while there is some variation in the emission parameters for **1** in the different solvents examined, in general for this complex τ_{em} is longer and Φ_{em} is dramatically lower than observed for **2** and is typical for other (diimine)-Re^I(CO)₃L⁺ complexes.^{28,30,31} The comparatively high τ_{em} and low Φ_{em} values observed for **1** lead to very low k_f values which fall in the range 10–100 s⁻¹.

Transient absorption spectroscopy was carried out on **1** and **2** in several solvents to provide further information concerning the nature of the excited states that are populated by near-UV excitation. In all of the experiments described below, samples were excited by using the third harmonic output of a Q-switched Nd:YAG laser (355 nm, 10 ns fwhm, 10 mJ/pulse). Figure 2a

illustrates transient absorption spectra for phen complex **2** in argon degassed MeCN taken at delay times ranging from 0.02 to 3.2 μs following laser excitation. The spectra are characterized by broad, comparatively featureless absorption in the near-UV visible region. The transient absorption decays obey monoexponential kinetics with $\tau = 1.6$ μs , in excellent agreement with the τ_{em} for this complex in MeCN (Table 1). The concordance of the emission and transient absorption lifetimes strongly implies that the transient absorption spectra in Figure 2a can be assigned to the $d\pi(\text{Re}) \rightarrow \pi^*(\text{phen})$ ³MLCT state of **2**.

Figure 2b illustrates the transient absorption spectra of the free dppz ligand (**3**) in argon degassed MeOH solution at delay times ranging from 0 to 16 μs following laser excitation. A strongly absorbing transient is produced during the laser pulse which has a narrow absorption band in the near-UV with $\lambda_{\text{max}} \approx 390$ nm and a comparatively broader band in the visible with $\lambda_{\text{max}} \approx 460$ nm. This transient absorption decays over the 0–10 μs time domain and at later times a different transient absorption is observed which is characterized by $\lambda_{\text{max}} \approx 390$ nm and weak absorption throughout the visible. Global least-squares analysis of the transient absorption data indicates that the early time transient absorption decays with $\tau = 3.0$ μs , while the longer lived transient absorption is very persistent and decays with $\tau \geq 300$ μs . A transient absorption experiment carried out on **3** in MeOH/aqueous Tris buffer (1:1 v:v) gave essentially identical results as observed for the compound in MeOH.

A variety of polycyclic aromatic hydrocarbons and heterocycles feature triplet excited states with lifetimes in the microsecond time domain and triplet–triplet absorption in the mid-visible region.⁴⁰ For example, phenazine in CF₃CH₂OH exhibits a triplet–triplet absorption maximum at 457 nm and the triplet state lifetime is $\tau = 170$ μs .^{40,41} On this basis, the transient that is observed at early times in the transient absorption spectrum of **3** (e.g., $\lambda_{\text{max}} = 390$ and 460 nm) and which decays with $\tau = 3.0$ μs is assigned to the triplet excited state of the dppz chromophore. At the present time the species responsible for the transient absorption that persists for $\tau \geq 300$ μs is uncertain; however, speculation as to its origin will be provided in the discussion section.

Figure 3a shows the transient absorption spectra for **1** in MeOH at delay times ranging from 0 to 40 μs following laser excitation. There are several features that are of interest with respect to these data. First, the transient observed immediately following laser excitation displays an absorption with a maxi

(40) Carmichael, T.; Hug, G. L. *J. Phys. Chem. Ref. Data* **1986**, *15*, 1.

(41) Del Barrio, J. I.; Rebato, J. R.; G-Tablas, F. M. *Chem. Phys. Lett* **1988**, *149*, 150.

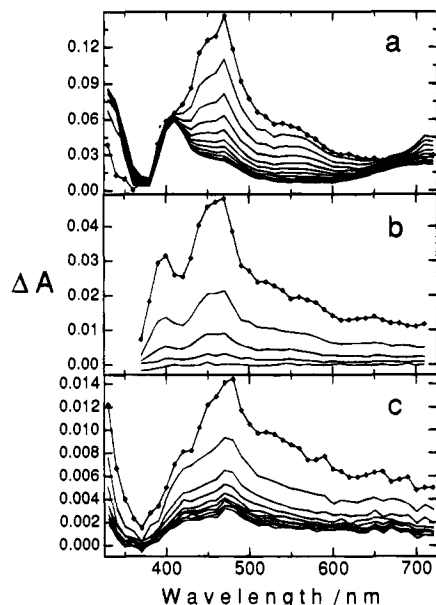


Figure 3. Transient absorption-difference spectra taken at various delay times following 355-nm laser excitation. In every set of spectra, the spectrum that is identified with point markers corresponds to 0 delay following the laser pulse. (a) Complex **1** in MeOH solution, $c = 50 \mu\text{M}$. Delay times range from 0 to 40 μs . (b) Complex **1** ($c = 50 \mu\text{M}$) in aqueous 25 mM Tris buffer. Delay times range from 0 to 160 ns. (c) Complex **1** ($c = 47 \mu\text{M}$) in aqueous 25 mM Tris buffer with [DNA] = 705 μM ([DNA]/[**1**] = 15). Delay times range from 0 to 8 μs .

mum at 470 nm with weak absorption in the near-UV region. Over the 0–20 μs time regime, the initial spectrum evolves into one having moderate absorption in the near-UV ($\lambda < 350 \text{ nm}$) and a maximum at 410 nm in the visible. Global least-squares analysis³⁹ of the multiwavelength transient absorption kinetic data indicates that the 470-nm transient, which is formed promptly after excitation, decays with $\tau = 12.7 \mu\text{s}$, while the transient observed at later times grows-in with the same lifetime. The correspondence between the lifetimes of the decay and grow-in processes strongly implies that the transient that is observed at long delay times is generated in a first-order reaction from the species that is produced initially by photoexcitation.

Time-resolved spectroscopic features that are very similar to those found for **1** in MeOH were observed when transient absorption experiments were carried out on the complex in argon degassed MeCN, MeCN/H₂O (95:5 v/v), 2-propanol (2-PrOH), *tert*-butyl alcohol (*t*-BuOH), and dichloromethane (CH₂Cl₂). Global analysis of the transient absorption data in these solvents indicates that the early time transient decay (and grow-in process) occurs with $\tau = 2.2 \mu\text{s}$ in CH₃CN and MeCN/H₂O (95:5 v/v), $\tau = 15.4 \mu\text{s}$ in 2-PrOH, $\tau = 3.6 \mu\text{s}$ in *t*-BuOH, and $\tau = 5.3 \mu\text{s}$ in CH₂Cl₂.

Figure 3b illustrates transient absorption spectra of **1** in aqueous solution with 25 mM Tris buffer at delay times ranging from 0 to 160 ns following laser excitation. Immediately following the laser excitation pulse a transient is observed which is characterized by a broad absorption band in the mid-visible with $\lambda_{\text{max}} \approx 470 \text{ nm}$ and a weak band in the blue with $\lambda_{\text{max}} \approx 400 \text{ nm}$. This transient decays quite rapidly following first-order kinetics with $\tau = 106 \text{ ns}$.

Photophysics in Aqueous Buffer with Calf Thymus DNA. All experiments were carried out in an aqueous solution which contained 25 mM tris(hydroxymethyl)aminomethane (Tris) with pH = 7. Reported [DNA] correspond to [nucleotide] determined by using the absorption at 260 nm (see Experimental Section).³⁴ Solutions were degassed by gentle argon bubbling for all emission and transient absorption experiments.

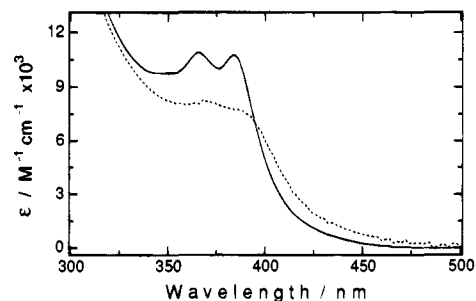


Figure 4. UV-visible absorption spectra of **1** ($c = 50 \mu\text{M}$) in aqueous 25 mM Tris buffer. Solid line: [DNA] = 0. Dashed line: [DNA] = 750 μM ([DNA]/[**1**] = 15).

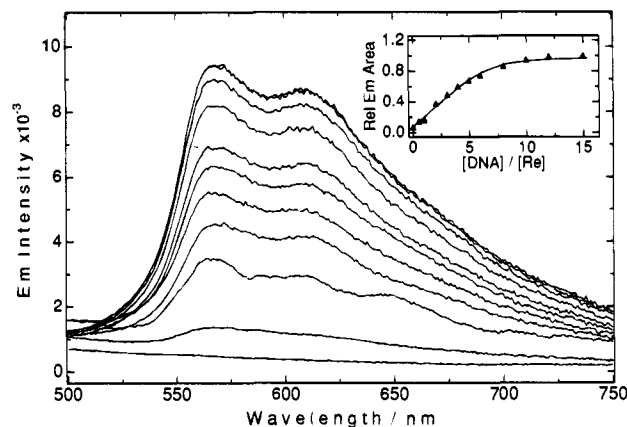


Figure 5. Emission spectra of **1** ($c = 32.5 \mu\text{M}$, $\lambda_{\text{ex}} = 350 \text{ nm}$) in degassed aqueous 25 mM Tris buffer at various DNA concentrations. [DNA]/[**1**] in order of increasing emission intensity: 0, 1.0, 2.0, 3.0, 4.0, 5.0, 6.0, 8.0, 10, 12, 15. Inset: Relative area under emission curves (500–750 nm) vs [DNA]/[**1**]. Solid lines through experimental points were calculated by using a Scatchard analysis with $K = 4 \times 10^6 \text{ M}$ and a binding site size of $n = 3.2$ base pairs.

UV-visible absorption spectra were obtained for aqueous buffer solutions of **1** ($c = 15.5 \mu\text{M}$) as a function of DNA concentration for [DNA]/[**1**] ranging from 0 to 15 and Figure 4 illustrates spectra in the 300–500-nm region for the solutions with [DNA]/[**1**] = 0 and 15. The spectrum of **1** in buffer without added DNA is very similar to that observed for the complex in methanol solution. However, addition of DNA induces hypochromism and a red shift of the near-UV absorption, which is dominated by the dppz bands (see Figure 4). The DNA-induced changes in the absorption occur gradually as [DNA]/[**1**] is increased from 0 to 12 and no other change is observed at higher [DNA]/[**1**].

Figure 5 illustrates steady-state emission spectra of **1** in degassed aqueous buffer solution ($c = 32.5 \mu\text{M}$) for [DNA]/[**1**] ranging from 0 to 15 (excitation wavelength is 350 nm for all emission experiments). In buffer solution alone ([DNA]/[**1**] = 0) emission is not observed in the 500–800-nm region ($\Phi_{\text{em}} < 0.00005$); however, addition of DNA to the buffer solution induces a pronounced increase in the emission yield. The emission intensity increases as [DNA]/[**1**] increases from 0 to 12; however, further increases are not observed for [DNA]/[**1**] > 12. This effect is illustrated clearly by the inset in Figure 5, where the relative area under the emission curve (e.g., the relative emission yield) is plotted as a function of [DNA]/[**1**]. Comparison of Figures 1 and 5 reveals that emission from **1** in the presence of DNA is similar in energy and bandshape to emission from the complex in MeOH, which strongly implies that the emission emanates from the same excited state in these two solution environments. The emission quantum yield and lifetime(s) for **1** in aqueous solution with [DNA]/[**1**] = 15 are

listed in Table 1. As can be seen from these data, the overall emission properties at high [DNA]/[1] are comparable to those observed when the complex is in organic solvents, with the exception that the emission decay is multiexponential when the complex is bound to DNA. Detailed studies of the emission decay kinetics of **1** as a function of [DNA] were precluded owing to the low quantum efficiency (and low radiative rate) for the emission.

Figure 3c illustrates transient absorption spectra of **1** ($c = 47 \mu\text{M}$) in aqueous buffer solution with [DNA]/[1] = 15 at delay times ranging from 0 to 8 μs following laser excitation. The time-resolved spectroscopic data reveal that a transient is formed during the laser pulse which has a maximum at 480 nm. Global analysis of the transient absorption data reveals that the transient which is initially formed by photoexcitation decays uniformly at all wavelengths. Importantly, in contrast to observations in organic solvents, a second transient is *not observed* at later delay times for aqueous buffer solutions of **1** in the presence of DNA. However, global least-squares kinetic analysis reveals that the transient absorption decays following biexponential kinetics, with $\tau_1 = 620 \text{ ns}$ ($\alpha_1 = 0.67$) and $\tau_2 = 10 \mu\text{s}$ ($\alpha_2 = 0.33$).

The 480 nm transient absorption decay kinetics of **1** ($c = 47 \mu\text{M}$) in aqueous buffer solutions were measured for [DNA]/[1] ranging from 0 to 15. Analysis of the single wavelength kinetic traces indicates that in each case the decays do not follow single exponential kinetics, consistent with the global kinetic analysis of the multiwavelength data for **1** at [DNA]/[1] = 15. At each [DNA]/[1] that was examined, the single wavelength decays could be simulated very well using a biexponential expression of the form

$$\Delta A^{480 \text{ nm}}(t) = \alpha_1 \exp\left(-\frac{t}{\tau_1}\right) + \alpha_2 \exp\left(-\frac{t}{\tau_2}\right) \quad (1)$$

where α_1 and τ_1 are the normalized amplitude and decay lifetime, respectively, for the short-lifetime decay component and α_2 and τ_2 are the normalized amplitude and decay lifetime, respectively, for the long-lifetime decay component. In order to aid the data analysis a "median" lifetime ($\langle\tau\rangle$) was also calculated for each sample by using the following expression,

$$\langle\tau\rangle = \alpha_1\tau_1 + \alpha_2\tau_2 \quad (2)$$

A summary of the transient absorption decay data as a function of [DNA]/[1] is presented in Figure 6, where the upper plot (Figure 6a) shows the trends in the normalized amplitudes, and the lower plot (Figure 6b) illustrates the trends in the lifetimes. Several points are of note with respect to these data. As noted above, in the absence of DNA the transient absorption decays rapidly with $\tau = 106 \text{ ns}$. However, upon the addition of DNA to the solution the decay becomes biphasic and a comparatively long-lived decay component (τ_2) becomes readily apparent in the kinetic traces. The relative amplitude and lifetime of this long-lifetime component steadily increase as [DNA]/[1] increases. A concomitant increase in the lifetime of the short-lived component (τ_1) is also observed with increasing [DNA]/[1]; however, the relative contribution of this component to the overall decay kinetics becomes less significant.

The overall change in the transient absorption decay kinetics of **1** as a function of [DNA]/[1] is reflected by the behavior of $\langle\tau\rangle$; note that this parameter increases substantially as [DNA]/[1] increases from 0 to 8, and then more-or-less levels off at higher [DNA]/[1]. Interestingly, the dependence of the median transient absorption lifetime ($\langle\tau\rangle$) on [DNA]/[1] parallels the dependence of the relative emission yield on [DNA]/[1] (compare inset to Figure 5 with Figure 6b). Furthermore, the

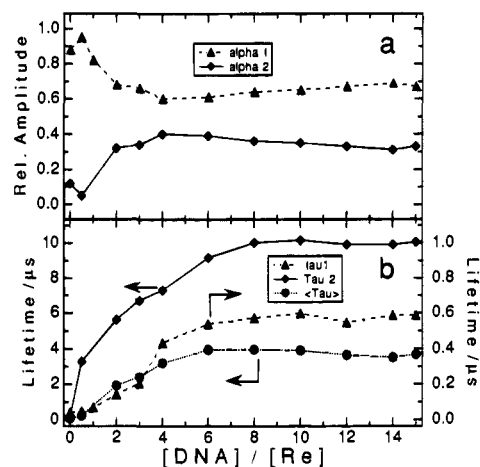


Figure 6. Graphical analysis of transient absorption decay kinetics of **1** in aqueous 25 mM Tris buffer as a function of [DNA]/[1]. (a) Plots of normalized decay component amplitudes: \blacktriangle , α_1 ; \blacklozenge , α_2 . (b) Plots of decay lifetimes; \blacktriangle , τ_1 ; \blacklozenge , τ_2 ; \bullet , $\langle\tau\rangle$. Note that the y-axis for τ_1 is on the right-hand side and the y-axis for τ_2 and $\langle\tau\rangle$ is on the left-hand side.

transient absorption and emission decay lifetimes of **1** at [DNA]/[1] = 15 are in reasonable agreement. These two features strongly imply that the excited state of **1** which is observed by transient absorption spectroscopy is the same as the one that is responsible for the emission that is observed when the complex is bound to DNA.

Discussion

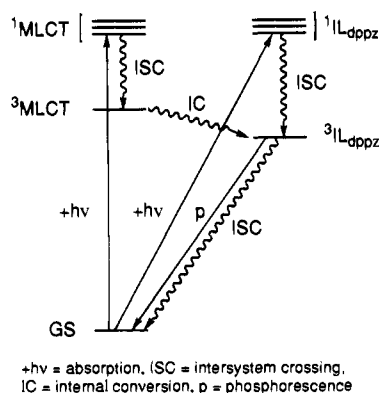
Concerning the Nature of the Lowest Excited States of 1 and 2 in Homogeneous Solution. The photophysics of complexes of the type *fac*-(diimine) $\text{Re}^{\text{I}}(\text{CO})_3\text{L}$, where diimine is a polypyridine ligand such as 2,2'-bipyridine (bpy) or 1,10-phenanthroline (phen), and L = halide, substituted pyridine, nitrile, or isonitrile, have been the subject of intensive photophysical investigation.^{28–31} Based on the results of these investigations it is possible to make generalizations concerning the nature of the lowest excited states and luminescence properties of this family of complexes. First, except in unusual situations, the energetically lowest lying excited state is based on $d\pi(\text{Re}) \rightarrow \pi^*$ (diimine) $^3\text{MLCT}$. The $^3\text{MLCT}$ states are characterized by several features which include to following:^{28–31} (1) broad, structureless luminescence in fluid solutions with λ_{max} in the range 500–650 nm; (2) moderate emission yields (Φ_{em} ranging from 0.01 to 0.3); (3) excited state lifetimes ranging from 0.02 to 2 μs ; and (4) radiative decay rate constants ranging from 10^5 to 10^6 s^{-1} and non-radiative decay rate constants ranging from 10^6 to 10^7 s^{-1} . However, well-documented examples exist in which the lowest excited state of a (diimine) $\text{Re}^{\text{I}}(\text{CO})_3\text{L}$ complex is based on an intraligand $^3\pi,\pi^*$ transition of the diimine ligand ($^3\text{IL}_{\text{diimine}}$).^{42–44} This situation occurs when the $^3\pi,\pi^*$ state of the diimine lies at a lower energy compared to the $d\pi(\text{Re}) \rightarrow \pi^*$ (diimine) $^3\text{MLCT}$ manifold.^{42,43} It is often easy to identify cases where $^3\text{IL}_{\text{diimine}}$ is the lowest lying excited state by the following features:⁴³ (1) existence of well-resolved vibronic structure in the emission in fluid solution; (2) abnormally low radiative rate constant; and (3) the transient absorption spectrum does not display features characteristic of the diimine radical anion.

(42) Sacksteder, L. A.; Lee, M.; Demas, J. N.; DeGraff, B. A. *J. Am. Chem. Soc.* **1993**, *115*, 8230.

(43) Shaw, J. R.; Schmehl, R. H. *J. Am. Chem. Soc.* **1991**, *113*, 389.

(44) Shaw, J. R.; Webb, R. T.; Schmehl, R. H. *J. Am. Chem. Soc.* **1990**, *112*, 1117.

Scheme 1



With this background in mind, the photophysical results on phen complex **2** provide strong evidence that the lowest excited state is based on $d\pi(\text{Re}) \rightarrow \pi^*(\text{phen})$ $^3\text{MLCT}$. First, the emission appears as a broad structureless band (Figure 1). Second, the emission parameters Φ_{em} , τ_{em} , and k_{r} are typical of those expected for an $^3\text{MLCT}$ state in a d^6 transition metal complex.^{28–31} Finally, the transient absorption spectrum is consistent with that expected for a d^6 metal \rightarrow phen $^3\text{MLCT}$ excited state.⁴⁵

The photophysical properties of dppz complex **1** in organic solvents contrast sharply with those of phen complex **2**. This difference leads to the conclusion that the lowest excited state of **1** is an intraligand n,π^* or π,π^* triplet state which is based on the dppz ligand ($^3\text{IL}_{\text{dppz}}$). This also implies that emission from the complex is $^3\text{IL}_{\text{dppz}}$ phosphorescence. This conclusion is supported by a number of facts. First, the $^3\text{IL}_{\text{dppz}}$ phosphorescence of **1** in MeOH appears as a band with two well-resolved vibronic features (Figure 1). The spacing between the two vibronic bands in the phosphorescence (1260 cm^{-1}) matches the spacing of the two vibronic bands that are resolved in the dppz intraligand absorption that dominates the near-UV absorption of the complex (1280 cm^{-1}). Second, Φ_{em} for **1** is 50- to 100-fold lower than that of **2**, despite the fact that τ_{em} is generally longer for **1**. The combination of low Φ_{em} and long τ_{em} leads to a very low k_{r} for **1**, which is consistent with the $^3\text{IL}_{\text{dppz}}$ assignment for the emission. Similar low k_{r} values are observed for other d^6 transition metal complexes which phosphoresce from ^3IL states at room temperature in fluid solution.^{43,44} Third, and perhaps most convincing, is the fact that the transient absorption spectrum of **1** is substantially unlike that of **2**, but very similar to the transient absorption spectrum of the free dppz ligand **3** (compare Figures 2b and 3a) which has been assigned to the triplet excited state of the dppz chromophore.⁴⁶

A summary of the photophysics of **1** in organic solvents is provided by the Jablonski diagram in Scheme 1. Near-UV excitation of the complex initially populates states having $^1\text{MLCT}$ and $^1\text{IL}_{\text{dppz}}$ character. Internal conversion and intersystem crossing pathways lead exclusively to the lowest lying state which has $^3\text{IL}_{\text{dppz}}$ character. Sufficient data are not available to determine whether the low-lying $^3\text{IL}_{\text{dppz}}$ state has a $^3n,\pi^*$ or $^3\pi,\pi^*$ configuration. In any case, the $^3\text{IL}_{\text{dppz}}$ state

relaxes by radiative (phosphorescence) and non-radiative (intersystem crossing) pathways to the ground state.

While it is clear that the lowest excited state of **1** in organic solvents is $^3\text{IL}_{\text{dppz}}$, there remain several anomalous features concerning the photophysics of the complex which must be addressed. First, the transient absorption and emission studies indicate that the excited state of **1** decays 10 to 100 times faster in aqueous solution than in organic solvents. Second, the transient absorption studies of **1** in organic solvents and **3** in MeOH and MeOH/aqueous buffer (1:1 v/v) indicate the presence of an unidentified transient which has a lifetime in excess of $300\text{ }\mu\text{s}$. We first turn to a discussion of the origin of the quenching of the excited state of **1** in aqueous solution. The second issue is considered in the next section.

A number of recent studies have examined the photophysics of complexes of the type $(\text{L})_2\text{Ru}(\text{dppz})^{2+}$ and $(\text{L})_2\text{Os}(\text{dppz})^{2+}$, where L = 2,2'-bipyridine or 1,10-phenanthroline.^{17–21,23} In these systems, the lowest excited state is based on a $d\pi(\text{M}) \rightarrow \pi^*(\text{dppz})$ $^3\text{MLCT}$ transition. The $^3\text{MLCT}$ assignment is unambiguous in these systems owing to the comparatively lower oxidation potentials of Ru(II) and Os(II) relative to Re(I).⁴⁷ The lower oxidation potentials effectively decrease the energy of the $^3\text{MLCT}$ manifold relative to the energy of $^3\text{IL}_{\text{dppz}}$. Studies of the Ru(II)– and Os(II)–dppz complexes indicate that the $\text{M} \rightarrow \text{dppz}$ $^3\text{MLCT}$ state is quenched by protic solvents such as H_2O and alcohols.^{19,20} The mechanism for the $^3\text{MLCT}$ quenching is believed to be proton transfer (or H-bond formation) between the solvent and one of the phenazine nitrogens which are basic due to the anion radical character of the dppz acceptor ligand in the $^3\text{MLCT}$ state.^{19–21} These studies also demonstrate that the lifetime of $^3\text{MLCT}$ is enhanced when the Ru(II)– or Os(II)–dppz complexes bind to DNA via intercalation. The increase in $^3\text{MLCT}$ lifetime concomitant with intercalation of the complex is believed to arise because the intercalated dppz ligand is inaccessible to H_2O .

A similar situation would be expected to ensue for the $d\pi(\text{Re}) \rightarrow \pi^*(\text{dppz})$ $^3\text{MLCT}$ state in **1**. Thus, $^3\text{MLCT}$ should be strongly quenched in protic solvents such as H_2O . However, the luminescence and transient absorption studies indicate that the lowest excited state of **1** is $^3\text{IL}_{\text{dppz}}$. Because this intraligand excited state is based on either an n,π^* or π,π^* transition, it is not expected to be quenched by proton transfer. Indeed, consistent with this premise, our work shows that the triplet state of **3** has essentially the same lifetime in MeOH and MeOH/ H_2O (1:1 v/v) thereby demonstrating that H_2O does not quench the dppz triplet.

The various photophysical observations for **1** and **3** lead to the inescapable conclusion that in **1** there exists a mechanism by which H_2O quenches the $^3\text{IL}_{\text{dppz}}$ state that is *unique to the metal complex* and does not operate in the free dppz ligand. A clue to the apparently unique behavior of **1** in aqueous solution is that in the complex the energy of the $d\pi(\text{Re}) \rightarrow \pi^*(\text{dppz})$ $^3\text{MLCT}$ state is only slightly above that of $^3\text{IL}_{\text{dppz}}$. This is evident because the $^3\text{IL}_{\text{dppz}}$ emission of **1** and the $^3\text{MLCT}$ emission of **2** overlap quite nicely in MeOH (see Figure 1). Because of the relatively close energetic proximity of $^3\text{MLCT}$ and $^3\text{IL}_{\text{dppz}}$ in **1**, the $^3\text{MLCT}$ manifold will provide a pathway for deactivation of $^3\text{IL}_{\text{dppz}}$ via an (endothermic) internal conversion process. Furthermore, since the energy of the relaxed $^3\text{MLCT}$ decreases with increasing solvent polarity⁴⁸ $^3\text{IL}_{\text{dppz}} \rightarrow ^3\text{MLCT}$ internal conversion will occur more rapidly in solvents

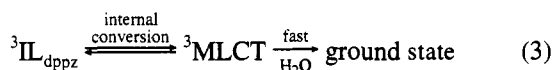
(45) Ohno, T.; Yoshimura, A.; Prasad, D. R.; Hoffman, M. Z. *J. Phys. Chem.* **1991**, *95*, 4723.

(46) It is notable that the strong transient absorption feature at 390 nm in the spectrum of the free dppz ligand **3** is not apparent in the spectrum of metal complex **1**. There are several possible reasons for this difference. First, the metal complex likely has stronger ground-state bleaching in this region, which will partially offset the absorption feature. Second, it is possible that the electronic configuration of the triplet state (e.g., n,π^* vs π,π^*) may be changed by complexation of the metal at the pyrido nitrogens.

(47) Caspar, J. V. Ph.D. Dissertation, University of North Carolina at Chapel Hill, 1983.

(48) The $^3\text{MLCT}$ emission maximum of **2** red-shifts as the solvent polarity increases while the $^3\text{IL}_{\text{dppz}}$ phosphorescence maximum of **1** is relatively invariant with solvent polarity (see Table 1).

of high polarity. Coupled with the fact that the $^3\text{MLCT}$ state of **1** is anticipated to be short lived in H_2O due to proton-transfer quenching, the energetically close-lying $^3\text{MLCT}$ state will provide a funnel for comparatively rapid deactivation of the lowest lying $^3\text{IL}_{\text{dppz}}$ state in H_2O :



The fact that the effect of solvent on the energy of $^3\text{MLCT}$ relative to $^3\text{IL}_{\text{dppz}}$ plays an important role with respect to the quenching that is observed in H_2O is supported by the observation that the $^3\text{IL}_{\text{dppz}}$ state of **1** is not quenched in $\text{CH}_3\text{-CN}$ with 5% added H_2O ($[\text{H}_2\text{O}] = 2.7 \text{ M}$). The lack of observable quenching at this high H_2O concentration indicates that quenching does not occur by a dynamic process. Rather, it implies that quenching requires that **1** be completely solvated by H_2O in order for quenching to occur. This behavior is distinctly different from that of $(\text{phen})_2\text{Ru}(\text{dppz})^{2+}$, which is quenched dynamically by H_2O at concentrations as low as 0.5 M in CH_3CN solution.^{20b}

Finally, assuming that the model presented above is correct, it is worthwhile to note that the $^3\text{MLCT}$ manifold plays a similar role in influencing the photophysics of the $^3\text{IL}_{\text{dppz}}$ state in **1** compared to the role played by the $^3\text{d-d}$ manifold in influencing the photophysics of the $^3\text{MLCT}$ state in polypyridine $\text{Ru}(\text{II})$ complexes.^{47,49-52} Specifically, detailed experiments have shown that in polypyridine $\text{Ru}(\text{II})$ complexes the $^3\text{d-d}$ manifold lies some $1000\text{--}4000 \text{ cm}^{-1}$ above the lowest-lying (luminescent) $^3\text{MLCT}$ state.⁴⁹⁻⁵² In the $\text{Ru}(\text{II})$ systems, the $^3\text{d-d}$ state is very short lived; therefore, thermally activated $^3\text{MLCT} \rightarrow ^3\text{d-d}$ internal conversion is irreversible and is an important deactivation pathway for $^3\text{MLCT}$ at temperatures near ambient. Of direct relevance to the present study is that the rate of $^3\text{MLCT} \rightarrow ^3\text{d-d}$ internal conversion in $\text{Ru}(\text{II})$ polypyridine complexes increases as the polarity of the solvent decreases, which is due to the increase in the energy of $^3\text{MLCT}$ relative to $^3\text{d-d}$ with decreasing solvent polarity.^{47,49}

Concerning the Nature of the Long-Lived Transient Observed by Flash Photolysis. While the early time transient observed in transient absorption spectroscopy of **1** and **3** is easily identified as the triplet state of the dppz chromophore, in most cases flash photolysis of these two compounds produces a transient with a significantly longer lifetime than the triplet state and which has a near-UV/visible difference spectrum that is distinct from that of the dppz triplet state. Principal component analysis has been carried out to calculate the difference spectra of the two kinetically distinct species observed in the time-resolved data (Figures 7a and 7b).³⁹ For both compounds, at early times the time-resolved spectra are dominated by the absorption that has been assigned to the triplet state of the dppz chromophore (solid lines in Figures 7a and 7b). By contrast, the later time spectra of both **1** and **3** are virtually identical and are dominated by a transient that absorbs in the UV and in the visible (dashed lines in Figure 7a and 7b). For both **1** and **3** this transient decays with $\tau \approx 300 \mu\text{s}$. The long-lived transient is observed following flash photolysis of **1** in every homogenous solvent examined where the $^3\text{IL}_{\text{dppz}}$ triplet state has a lifetime longer than $2 \mu\text{s}$ (e.g., MeOH , 2-PrOH , $t\text{-BuOH}$, CH_2Cl_2 , and CH_3CN).

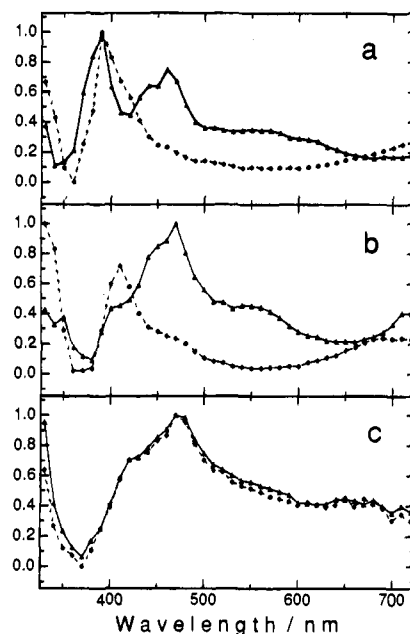


Figure 7. Transient absorption difference spectra of the principal spectral components extracted by global analysis of transient absorption data: (a) **3** in MeOH ; (b) **1** in MeOH ; (c) **1** in aqueous 25 mM Tris buffer with $[\text{DNA}]/[\text{1}] = 15$. In each set of spectra the solid line is the principal component spectrum of the species which predominates at early delay times, and the dashed line is the principal component spectrum of the species which predominates at later delay times.

Organic triplet states are well-known to be very reactive with respect to H-atom abstraction.⁵³ Based on this fact, we first hypothesized that the long-lived intermediate is likely the radical that would be produced if the dppz triplet state abstracts a H-atom from a solvent molecule. However, several experiments that have been performed rule out this possibility. First, transient absorption studies of **1** indicate that the long-lived transient is produced with comparable efficiency in every solvent examined—despite the fact that some solvents are much better H-atom donors than others. Secondly, if the long-lived transient is produced by H-atom abstraction from the solvent by the dppz triplet state, the triplet decay kinetics would be anticipated to exhibit a deuterium isotope effect. This is not the case: the lifetime of the $^3\text{IL}_{\text{dppz}}$ state is the same within experimental error in CH_3OH and CD_3OD . Third, and perhaps most convincingly, a flash photolysis/Fourier transform electron paramagnetic resonance (FT-EPR) experiment that was carried out on **3** in 2-PrOH ($c = 1 \times 10^{-3} \text{ M}$) showed no evidence for a free radical intermediate.^{54,55} Since this technique has sufficient sensitivity to detect radicals at micromolar or lower concentration,⁵⁵ we are forced to conclude that H-atom abstraction by the dppz triplet state is not an important excited state decay process.

The data which are presently available point to the possibility that the long-lived transient is the product of a valence isomerization of the dppz chromophore. Furthermore, this product is formed via decay of the dppz triplet excited state. These conclusions are based on several indirect experimental observations: (1) The transient is observed for both metal complex **1** and **3**. (2) The transient is observed in a wide spectrum of solvents including those that are protic, non-protic, and poor H-atom donors. (3) The transient is formed comparatively rapidly in very dilute solutions precluding the

(49) Caspar, J. V.; Meyer, T. J. *J. Am. Chem. Soc.* **1983**, *105*, 5583.

(50) Caspar, J. V.; Meyer, T. J. *Inorg. Chem.* **1983**, *22*, 2444.

(51) Meyer, T. J. *Prog. Inorg. Chem.* **1983**, *30*, 389.

(52) Wacholtz, W. F.; Auerbach, R. A.; Schmehl, R. H. *Inorg. Chem.* **1986**, *25*, 227.

(53) Turro, N. J. *Modern Molecular Photochemistry*; Benjamin-Cummings: Menlo Park, 1979.

(54) van Willigen, H.; Leustein, P. R.; Ebersole, M. H. *Chem. Rev.* **1993**, *93*, 173.

(55) Leustein, P. R.; van Willigen, H. *J. Chem. Phys.* **1991**, *95*, 900.

possibility that it is produced in a bimolecular reaction. (4) In the UV region, a clear transient absorption rise is observed which displays the same kinetics as the triplet decay. (5) The transient is not formed for **1** in H₂O (under these circumstance the ³IL_{dppz} state is strongly quenched). We prefer not to speculate on the structure of the valence isomerization product at the present time; experiments in progress seek to provide conclusive evidence concerning the structure of the intermediate.

Photophysics of 1 in the Presence of DNA. The spectroscopic information gathered on **1** in aqueous buffer solution in the presence of varying amounts of calf thymus DNA indicates that the complex binds to the polymer. Furthermore, as outline below, the data suggest that intercalation is the primary mechanism for binding of **1** to DNA.

First, binding parameters for **1** to DNA were determined from the relative change in emission yield as a function of [DNA]/**1** by using a Scatchard analysis and assuming a single type of binding site. The best fit to the experimental emission yield data was obtained with a site-covering size of $n = 3.2$ base pairs and a binding constant of $K = 6.0 \times 10^5 \text{ M}^{-1}$ (see Figure 5, inset, for comparison of calculated and experimental data). The calculated binding constant for **1** is lower than the binding constant of (bpy)₂Ru(dppz)²⁺ ($K = 4 \times 10^6 \text{ M}^{-1}$).^{15c,19} However, the diminished binding constant for **1** relative to (bpy)₂Ru(dppz)²⁺ can be accounted for almost entirely by the difference in the charge of the complexes: the Ru(II) complex is a dication while Re(I) complex **1** is a monocation. Calculations based on polyelectrolyte theory suggest that the "intrinsic" or "non-electrostatic" binding constants for **1** and (bpy)₂Ru(dppz)²⁺ differ by no more than a factor of 2.^{15c} The rather close correspondence between the "non-electrostatic" binding constants for the Re(I) and Ru(II) dppz complexes, while not surprising, suggests that they share a common binding motif (e.g., intercalation of the dppz moiety).

The second important observation which supports the premise that **1** binds to DNA via intercalation is the observation of substantial hypochromism and a red-shift in the near-UV absorption features that are due primarily to the dppz chromophore.⁵⁶ These changes in the absorption indicate that there is a strong interaction between the dppz ligand and the polymer, as anticipated if binding occurs by intercalation.⁵⁶

Complex **1** is non-luminescent in degassed aqueous buffer solution, but it is moderately luminescent when it binds to DNA. The emission from the DNA-bound form is very similar to that observed when the complex is in MeOH (compare Figures 1 and 5) which implies that emission from the DNA-bound complex can be assigned as ³IL_{dppz} phosphorescence. This hypothesis is further substantiated by the following observations: (1) The transient absorption spectrum of DNA-bound **1** (Figure 3c) is virtually identical to the early-time transient absorption spectra seen for the complex in MeOH and MeCN solutions which have been attributed to ³IL_{dppz}. (2) There is reasonable agreement between the emission and transient absorption decay kinetics for DNA-bound **1**. (For [DNA]/**1** = 15: emission, $\tau_1 = 170 \text{ ns}$ ($\alpha_1 = 0.80$) and $\tau_2 = 13.5 \mu\text{s}$ ($\alpha_2 = 0.20$); transient absorption, $\tau_1 = 620 \text{ ns}$ ($\alpha_1 = 0.67$), $\tau_2 = 10 \mu\text{s}$ ($\alpha_2 = 0.33$)).

Prior to discussing the decay behavior of ³IL_{dppz} as a function of [DNA]/**1**, it is important to contrast the transient absorption behavior of the DNA-bound complex with that observed for the complex in organic solvents. At every [DNA]/**1** ratio examined, the transient absorption decay of **1** follows biexponential kinetics. Factor analysis of the time-resolved transient absorption spectra for **1** at [DNA]/**1** = 15 indicates that spectra

of the two principal transient absorption spectral components (Figure 7c) are superimposable. This analysis indicates that both the short-lived and the long-lived transient absorption components observed for the DNA-bound complex are due to the same species: ³IL_{dppz}. This situation contrasts with that for **1** in homogeneous organic solvents. In the homogeneous solvents, a very long-lived transient is observed which is tentatively assigned to the product of a valence isomerization of the dppz chromophore. That a similar transient intermediate is not formed when the DNA-bound form of **1** is photoexcited implies that the DNA-bound complex lies in an environment that is too constrained to accommodate the structural rearrangement that would likely accompany valence isomerization of the dppz ligand. This is consistent with the proposition that **1** binds to DNA via intercalation.

Because emission from **1** at low [DNA]/**1** is comparatively weak, detailed studies of the decay kinetics of ³IL_{dppz} as a function of [DNA]/**1** were effected by using transient absorption spectroscopy (Figure 6). As noted above, the lifetime of ³IL_{dppz} increases substantially when **1** binds to DNA. However, despite the substantial overall increase in lifetime with increasing [DNA]/**1**, the decay continues to obey biexponential kinetics with the long-lived component having a lifetime that is at least 10-fold larger than the short-lived component. Two questions concerning the decay kinetics must be addressed: (1) Why does the lifetime of ³IL_{dppz} increase when the complex binds to DNA? (2) Why are multiexponential kinetics observed for the decay of ³IL_{dppz} when the complex is bound to DNA?

The first point is explained by recalling that ³IL_{dppz} is quenched strongly in H₂O, presumably via solvent-induced quenching of the energetically close ³MLCT state (eq 1). It is very likely that this quenching pathway is shut down in the DNA-bound form of **1** for two reasons. First, in the bound complex the dppz ligand is less accessible (or inaccessible) to H₂O.^{19,20} Second, the comparatively lower polarity of the DNA binding site may raise the energy of ³MLCT relative to ³IL_{dppz} thereby slowing down ³IL_{dppz} to ³MLCT internal conversion. Interestingly, despite the fact that the lowest state of **1** is ³IL_{dppz}, the effect of DNA binding on the excited state lifetime of the complex is remarkably similar to that observed for the Ru(II)- and Os(II)-dppz analogs.^{19,20} This similarity underscores the fact that the same underlying mechanism is probably responsible for the luminescence "light switch" effect in all three systems (e.g., quenching of ³MLCT by H₂O).

The final point which must be considered concerns the origin of the biexponential decay kinetics observed for ³IL_{dppz} when **1** is bound to DNA. As background, it is important to note that multiexponential emission decay kinetics are typically seen for probe molecules that are bound to DNA.^{19,20,23} Heterogeneous decay kinetics are usually attributed to the existence of different types of binding sites along the DNA polymer. By analogy, we believe that the observation of two clearly resolved excited state decay components for DNA-bound **1** establishes that the DNA polymer provides more than one type of binding site for the complex. These two binding sites may differ with respect to the geometry of the intercalated dppz ligand relative to the DNA base pairs (e.g., side-on vs perpendicular relative orientations)²⁰ or with respect to chemical composition of the intercalation site(s). An interesting point to consider is that the short-lived decay component may be due to a binding site which exposes the complex to a relatively more polar environment. In this situation, the energy of the MLCT state may be lowered to such an extent that it can be populated by (endothermic) internal conversion from the ³IL_{dppz} state. As a result, the excited state decay kinetics for complexes in this site would be

controlled by the rate of ${}^3\text{IL}_{\text{dppz}} \rightarrow {}^3\text{MLCT}$ internal conversion, not by the comparatively slower non-radiative decay rate of the spin-forbidden triplet intraligand state.

Conclusion

Photophysical studies of Re(I)-dppz complex **1** in homogenous organic solvents indicate that the lowest excited state is ${}^3\text{IL}_{\text{dppz}}$. In degassed MeCN and MeOH, weak phosphorescence is observed from ${}^3\text{IL}_{\text{dppz}}$, and this excited state is readily detected by its characteristic and strong $T_0 \rightarrow T_n$ absorption. No luminescence is observed from **1** in aqueous Tris buffer; however, when bound to DNA, presumably via intercalation, the complex is moderately luminescent. The similarity of the emission and transient absorption features of **1** in homogenous organic solution and in the presence of DNA in aqueous solution indicates that emission from the DNA-bound complex emanates

from ${}^3\text{IL}_{\text{dppz}}$. The difference in the photophysical properties of **1** and the Ru(II)- and Os(II)-dppz analogs arises because the $d\pi(M) \rightarrow \pi^*(\text{dppz})$ ${}^3\text{MLCT}$ state(s) are at higher energy in the Re(I) system thereby allowing the low-lying dppz-based intraligand triplet state(s) to dominate the photophysics of the system.

Acknowledgment is made to the donors of the Petroleum Research Fund, administered by the American Chemical Society, for partial support of this work. H.D.S. was a student participant in the National Science Foundation Research Experiences for Undergraduates Site at the University of Florida (Grant No. CHE-9200344). We thank Professor Hans van Willigen for performing the flash photolysis FT-EPR experiment on **3** at the University of Massachusetts at Boston.

JA943678L